Journal Pre-proof

Mobile laser scanning in support of national and regional forest inventories

Justin Holvoet, Nicolas Latte, Jérôme Perin, Jean-François Bastin, Hugo de Lame, Daniel Kükenbrink, Philippe Lejeune

PII: S2666-0172(25)00122-1

DOI: https://doi.org/10.1016/j.srs.2025.100316

Reference: SRS 100316

To appear in: *Science of Remote Sensing*

Received Date: 16 July 2025

Revised Date: 13 October 2025

Accepted Date: 14 October 2025

Please cite this article as: Holvoet, J., Latte, N., Perin, J., Bastin, J.-F., de Lame, H., Kükenbrink, D., Lejeune, P., Mobile laser scanning in support of national and regional forest inventories, *Science of Remote Sensing*, https://doi.org/10.1016/j.srs.2025.100316.

Mobile laser scanning in support of national and regional forest inventories

Justin Holvoet[a,*], Nicolas Latte[a], Jérôme Perin[a], Jean-François Bastin[a], Hugo de Lame[a], Daniel Kükenbrink[b], Philippe Lejeune[a]

[a]Liège University, Faculty of Gembloux Agro-Bio Tech; Passage des Déportés, 2, 5030 Gembloux, Belgique

[b]Swiss Federal Institute for Forest, Snow and Landscape Research WSL, Zurichstrasse 111, Birmensdorf, 8903, Switzerland

[*]**Correspondence**: J.holvoet@uliege.be

Abbreviations: NFI, national forest inventories; RFI, regional forest inventories; MLS, mobile laser scanning; ULS, unmanned laser scanning; DBH, diameter at breast height; TLS, terrestrial laser scanner; SLAM, simultaneous localisation and mapping; CBH, circumference at breast height; QSMs, quantitative structural models; RMSE, root mean square error

Abstract

In the context of a growing need to diversify forest information, national and regional forest inventories (NFI and RFI) could benefit from mobile Light Detection and Ranging (LiDAR) technologies. Ground-based mobile laser scanning (MLS) and unmanned aerial laser scanning (ULS) can potentially retrieve a large panel of forest attributes quickly, efficiently, and accurately. In this study, conducted in Wallonia (southern Belgium), we aimed to evaluate, in the context of an NFI, the accuracy of MLS at tree, plot, and inventory levels and the potential benefits of fusing ULS with MLS. In total, 60 circular forest plots of 0.1 ha containing 2,497 trees were measured by traditional inventory means and scanned using MLS. Among them, 27 were additionally scanned by ULS, and ULS and MLS scans were fused to produce an enhanced point cloud. We then evaluated the accuracy of MLS considering, at tree level, the diameter at breast height, total height, merchantable wood volume, and crown projected area and volume; at plot level, the total merchantable wood volume, number of trees, and total basal area; and for the whole inventory, the total volume and number of trees. Tree, plot, and inventory metrics were accurately acquired with a strong correlation to field measurements (r^2 ranging from 0.83 to 0.98). Out of all estimated metrics, height has a potential accurately estimated by MLS than by field measurements. The fusion of ULS and MLS allowed for a more accurate crown measurement, but height estimation was not significantly better than with MLS scan alone. The accuracy of soft- and hardwood forest plot estimations differed considering total plot wood volume, number of trees, and individual tree height. In this study, we explored the possibility and limitations of MLS in undertaking large-scale inventory in terms of accuracy, time, and reliability.

Keywords: Mobile laser scanning; Unmanned laser scanning; National forest inventory

1. Introduction

1.1 Context

Forest ecosystems account for a third of European land. Many countries have established national or regional forest inventories (NFI or RFI) to monitor the state of their forests and implement national forest policies. By using sampling plots scattered systematically over their territory, forest management institutions can assess the state and evolution of their forests over large areas (Rondeux et al., 2010). The first instance of NFIs in Europe can be traced back to the late 1910s in the Nordic countries (Tomppo et al., 2010), while most of the rest of European countries set theirs between 1960 and 2000 (Vidal et al., 2016).

The first goal of these forest inventories was to monitor forest wood stock and potential supply as well as forest productivity (Loetsch et al., 1973). Over time, emphasis shifted to multipurpose surveys to cater for the new need for information on biodiversity, forest sanitary states, carbon stocks, and tree population regeneration (Corona et al., 2011).

Traditionally, forest inventories focus on direct measurements acquired in the field and estimates derived from them which are time- and labour-intensive (Luoma et al., 2017). Common metrics obtained during field surveys include, among others, diameter at breast height (DBH), tree total height, stand dominant height, forest cover, and tree density. Traditional tools for obtaining these metrics include callipers or measuring tape for DBH, and electronic clinometers or cross-staffs for tree height. Wood volume and biomass are generally estimated using local allometric models.

The recent requirement for multipurpose surveys often lead NFI to add new attributes measured on each plot, thus impacting the cost and time of the measurements. In addition, non-negligible inaccuracies and imprecisions can exist for some measurements or metrics. For instance, tree height mean error can be up to 5 m when using a clinometer (Stereńczak et al., 2019). These errors can be worsened by dense forest cover, intricate tree crowns, or operator error (Luoma et al., 2017).

To address these issues, forest inventories often rely partially on precision forestry, which "… uses modern tools and technology to get as much real information as it is possible to improve decision

making process and to ensure current goals of forest management" (Kovacsova and Antalova, 2010). In this domain, ground-based LiDAR technologies show promising trends, allowing for the accurate acquisition of a 3D reproduction of the scanned environment at a close range. The resulting point cloud can then be processed to extract desired forest metrics (Hopkinson et al., 2004; Calders et al., 2020).

Among these technologies, multi-scan terrestrial laser scanner (TLS) has been successfully used to estimate forest metrics at the tree and stand levels, including DBH and tree height (Huang et al., 2011), single tree biomass and volume (Yu et al., 2013), tree growth (Jin et al., 2021), stand-level volume (Astrup et al., 2014), and tree density and basal area (Tansey et al., 2009). However, a few obstacles remain in the implementation of TLS in a large-scale forest inventory context: extended data acquisition times, ranging from 45 to 80 min for 400-m² plots (Vandendaele et al., 2022); occlusion due to laser stopping at the nearest surface (Liang et al., 2012); and scanner weight and dimensions, which make it impractical for large area surveys or countrywide forest inventories (Di Stefano et al., 2021).

In the context of NFIs requiring a shorter acquisition time and better manoeuvrability, mobile laser scanning (MLS) balances usability and data accuracy (Liang et al., 2014; Vandendaele et al., 2022). Mobile laser scanners use a simultaneous localisation and mapping (SLAM) algorithm to allow continuous scanning while the operator moves through the plot. Due to the increased number of points of view during the scan, MLS typically offers reduced occlusion compared with TLS (Di Stefano et al., 2021). Combined with the 100-m range of the new generation of scanners, these elements indicate that MLS would be more suitable for regular use in large-scale inventories. Even if it is less precise than TLS, the "noisier and fuzzier" point cloud resulting from MLS—partially due to the propagation of positioning errors (Bauwens et al., 2016; Chen et al., 2019)—also allows to extract accurately diameters, tree height and stem volume (Cabo et al., 2018; Chen et al., 2019; Balenovic et al., 2020; Bienert et al., 2021).

Another interesting LiDAR application for forest inventories is unmanned laser scanning (ULS), which refers to the use of drones mounted with LiDAR. These technologies offer a fast and easy way to recover

high-density clouds for the upper part of the canopy. While they are mostly used to extract accurate tree height and crown diameter (Wallace et al., 2012; Vandendaele et al., 2021), the possibility of combining ground-based LiDAR and ULS has been recently explored (Yun et al., 2019; Polewski et al., 2019). Panagiotidis et al. (2022) showed a potential benefit of combining ground-based LiDAR with ULS to increase tree height measurement accuracy and crown completion. Schneider et al. (2019) showed that a drastic reduction in occlusion was possible by fusing ULS and TLS, thus allowing for more complete forest coverage. Fekry et al., (2022) fusing MLS and ULS point cloud, found little impact on crown area and volume estimations, but found a significant impact on height measurement. They also found that the impact was more significant for redwood than for poplar. While LiDAR data fusion can help with many application, Balestra et al. (2024a) suggested that the major challenge in remote sensing data fusion is the increased cost, time, and expertise required to acquire, process, and validate multiple datasets which can differ in resolutions, accuracies, or temporal coverages. These difficulties, combined with delays between data acquisition and delivery, can reduce the effectiveness of fused products, particularly in rapidly changing forest conditions.

Since most terrestrial LiDAR studies have focused on a single forest stand, a limited number of plots, and/or individual trees, applying such technologies for large-scale forest inventories still needs to be investigated.

1.2: Aims and research questions

In this study, we aimed to evaluate the accuracy of MLS at tree, plot, and at the whole inventory levels in the context of an RFI. We also aimed to evaluate the potential benefit of fusing ULS with MLS, particularly for crown characteristics (area and volume) and tree height. More specifically, considering 60 plots of the regional forest inventory of Wallonia (southern Belgium), field measurements (FMs), MLS, and MLS/ULS metrics were extensively compared at three levels: tree (DBH, height, volume, and crown area and volume), plot (plot total merchantable wood volume, number of trees, and basal area), and inventory (total volume and number of trees, DBH and height population structure).

2. Material and Methods

2.1. Study area and sites

The study was conducted in Wallonia, the southern part of Belgium, particularly in the Ardenne ecoregion. The area benefits from a temperate maritime climate with annual precipitation ranging from 1,153 to 1,219 mm and annual mean temperature ranging from 7.7 to 8.7 °C. The study site's elevation ranges from 351 to 614 m.

Wallonia's RFI (southern Belgium), which started in 1980, employs a 500 × 1,000 m grid to sample the territory systematically. Every cross section of the grid ending up in forested land is then visited and measured in the field.

In this study, we selected 60 plots from this RFI (see Fig. 1). The plots were selected among the most common hard- and softwood forest types of the region. Typical Forest profiles encountered in the study area are illustrated in figure 2 and the tree density encountered in the study sites are displayed in figure 3. The stands were situated in forest stands dominated by beech (*Fagus sylvatica)* and indigenous oaks (*Quercus patrea, Quercus robur)* for hardwood forests, and spruce (*Picea abies)* and Douglas fir (*Pseudotsuga menziesii)* for softwood forests. These four species represent 76% of the standing wood volume in Wallonia. All plots were located in public forests. Dominance, and per se forest type, was attributed to the species, or the group of species, that accounted for at least 80% of the stem measured in the plot. All plots belonged to the following forest types : Oak forest, Beech forest, Mixed oak and beech forest, Spruce forest, Douglas' fir forest, and Mixed Spruced and Douglas' fir forest. We systematically selected plots in these forest type to cover the following gradients: the altitude with a range of 351 to 614 m, tree density with a range of 108 to 1425 tree/ha and stand development stage with basal area per hectare ranging from 3.37 to 45.62 m^2/ha. All study sites' slope ranged from 4.10° to 24.3°. The number of plots per forest structure is displayed in table 1.

Table 1: Number of plots per forest structure

FOREST STRUCTURE	PLOTS
SINGLE LAYERED FOREST	24
UNEVEN AGED FOREST	24
YOUNG PLANTATIONS	9
COPPICE UNDER SINGLE LAYERED FOREST	3

2.2. Field measurements

All 60 selected plots were re-inventoried before scanning. Contrary to the RFI using concentric sub-plots (Rondeux et al., 2010), all trees of at least 20 cm in circumference at breast height (CBH) in an 18-m radius (~0.1 ha) were considered. Breast height was defined as 1.30 m above ground. FMs consisted of DBH, tree position (azimuth and distance from the centre), species, and tree height. DBH was derived from CBH measurements, which were obtained using a measuring tape. Tree position was obtained using a compass for the azimuth and an electronic clinometer for the distance. Tree height was measured for at least 10 trees per plot using an electronic clinometer. The trees for height measurement were selected to cover the height range in each plot.

Merchantable wood volume is the volume of wood over bark contained in the stem between the first cut at the base of the trunk (+/- 10 cm above ground) up until a circumference of 22 cm. Merchantable wood volume over bark was estimated for each tree using Dagnelie's one-entry volume equation, which corresponded to the main stem's volume from the bottom up until a circumference of 22 cm. The equation uses CBH to estimate merchantable wood volume for individual trees (Dagnelie et al., 1999).

2.3. MLS and ULS

The plots were scanned using a ZEB-HORIZON mobile laser scanner (GeoSLAM, Ruddington, UK) during leaf-off conditions between January and March 2023 in both hard- and softwood forests. While the

leaf-off condition in softwood still lead to spruce and Dougla's fir to be foliated, it led to the absence of ground vegetation. The properties of the scanner can be found in table 1. The walking pattern is shown in Fig. 4. After testing different patterns, we settled for a circular, high-density walking pattern to minimise occlusion in the canopy. The scanning pattern comprised three steps: first, the scan started at the centre of the plot and began by circulating on a 22-m radius circle around the plot. Second, four "petals", each starting at the centre, reaching 22 m in a cardinal direction, circulating in the opposite direction of the 22-m circle and coming back to the centre of the plot, were adopted. Third, a smaller 15-m circle was applied before the scan ended at the centre of the plot. The MLS point cloud density varied from 33.337 to 84.063 point/m².

Additionally, 27 of the plots were concurrently scanned by ULS using a DJI Matrice300 drone (DJI Enterprise, Shenzhen, China) equipped with a DJI Zenmuse L1 scanner (DJI Enterprise). The properties of the scanner can be found in table 2. The drone followed three 50-m parallel transects over the plot, as illustrated in Fig. 5. The flight parameters included a 50% lateral overlap, a 100-m altitude from the take-off point, and a 10 m/s flight speed. The ULS point cloud density varied from 600 to 1,000 points/m² depending on the canopy complexity. These parameters were selected to obtain an easy to setup, fast, scan potentially implementable in NFI practices where time spent is a key factor. ULS and MLS point clouds were fused by first roughly aligning them manually by superposing the trees and ground points with CloudCompare translation and rotation tools. The precise co-regitration was then made using the fine registration Iterative Closest Point algorithm (ICP). (Fig. 6)

Table 2. ZEB Horizon RT and Dji Zenmuze L1 scanner specifications.

SCANNER	RANGE (m)	BEAM DIVERGENCE (mrad)	ACCURACY (cm)	MEASUREMENT RATE (point/sec)	WAVELENGTH (nm)
ZEB HORIZON RT	100	3.0	3	300.000	903
DJI ZENMUSE L1	450	0.52 (horizontal) * 4.9 (vertical)	3	240.000	905

2.4. Tree metrics

We extracted individual tree point clouds from the plot scans using Computree (Othmani et al., 2011) and the Simpleforest plugin (Hackenberg et al., 2021). This software was used for its user friendliness and for the convincing result of individual tree segmentation. We then calculated DBH, tree height, crown projected area and volume, and merchantable wood volume of each tree with a CBH of at least 20 cm. The individual point clouds were normalized by defining the lowest trunk point as z=0.

DBH was extracted using the method proposed by Terryn et al. (2023) by extracting 5-cm large slices along the z axis in the point cloud at 1.30 m height from the base of the trunk for each individual tree, fitting a circle on the trunk slice. The DBH was then extracted as the diameter of said circle. Tree height was computed as the difference between the minimal and maximal z coordinates of each tree point cloud. Crown projected area and volume were calculated using the ITSMe R package (Terryn et al., 2023). First, the crown points were identified as the points above the break point at which the mean distance of the points to the centre of the stem significantly increases (Schneider et al., 2020). The crown projected area corresponds to the convex hull of all the crown points projected on a plane parallel to the horizontal. The crown volume corresponds to the volume occupied by the alpha shape built around the crown points. The alpha value was set by default to 1. In our case, as the analysis was conducted on leaf-off hardwood stands, it was estimated that a larger alpha value would yield more reliable results. Smaller alpha values tend to fit fine branches too closely, which may result in underestimation when compared with leaf-on measurements. For softwoods, the results obtained with different alpha values were visually assessed, and no major differences were observed. This outcome is likely due to the more organized and denser structure of their crowns.

MLS merchantable wood volume was computed by reconstructing quantitative structural models (QSMs) (Raumonen et al., 2013) for every tree using the Matlab library TreeQSM and the method presented in the TreeQSM 2.4.1 manual (Raumonen & Akerblom, 2022). QSMs are a cylinder fitting method allowing trunk and branch reconstruction of the tree point cloud. The QSM was then truncated

196 to a threshold of 22 cm of circumference to keep only cylinders corresponding to the merchantable
197 wood volume, as illustrated in Fig. 7. The volume of these cylinders where then added up to estimate
198 the merchantable wood volume. Bias for all metrics was calculated as the difference between the
199 estimated value's mean and the reference value's mean. Root mean square error (RMSE) was also
200 calculated between measurement and reference value.

201

202 **2.5. Tree matching**

203 The trees individualised from the MLS and MLS/ULS were matched to FM ones according to their *XY*
204 coordinates and circumference, as illustrated in Fig. 8. The relative position of each individual tree point
205 cloud in the plot was obtained by identifying the coordinates (x,y) of the center of the convex hull build
206 around a 5cm thick slice of the stem extracted at 1.30m. Starting from the field identified trees with
207 the largest DBH to the smallest DBH, each of them was matched to the MLS identified tree with the
208 closest DBH within a radius of 2 meters.

209 **2.6. LiDAR and field comparisons**

210 We compared the MLS DBH and tree height with FM as well as MLS tree height with merged MLS/ULS
211 tree height. We also compared the crown projected area and volume from MLS and MLS/ULS.
212 Merchantable wood volume was estimated and compared for MLS and FM at both the tree and plot
213 levels. We further analysed the mean difference and standard deviation of each estimation between
214 MLS and FM for each tree species.

215 At the plot level, we compared aggregated estimates of volume and the total number of identified trees
216 and basal area from both FM and MLS. Total basal area was calculated as the sum of individual basal
217 area, which is the surface occupied by the tree trunk at 1.30 m above ground. The comparison between
218 plot level field measurements and the MLS estimations was based on all field measured trees against
219 all MLS detected trees regardless if the trees were matched or not.

220 At the whole inventory level, the total volume and number of trees were compared between MLS and
221 FM. The population structure, illustrated here as the cumulated frequency graph of the number of
222 individuals per diameter class for both DBH and tree height, was also constructed and compared.
223 Finally, we compared the total volume estimated by MLS and FM for each type of forest stand (cfr. Table
224 3).

225 **Table 3**. List of metrics estimated by the mobile laser scanning (MLS) survey, measurement level
226 (individual tree [Inv.], plot or whole inventory level), and comparison base for said metrics.

Metric	Level	Reference
DBH	Tree	FM
Height	Tree	FM
Height	Tree	MLS/ULS
Crown projected area	Tree	MLS/ULS
Crown volume	Tree	MLS/ULS
Wood Volume	Tree	FM
Wood Volume	Plot	FM
Total number of trees	Plot	FM
Total basal area	Plot	FM
Total Volume	Inv.	FM
Total Number of trees	Inv.	FM
DBH population structure	Inv.	FM
Height population structure	Inv.	FM

227 DBH, diameter at breast height; FM, field measurements; ULS, unmanned laser scanning.

3. Results

3.1 Field acquisition and processing time

The MLS and ULS acquisition times, as well as the processing time required for refining each plot point cloud, individual tree segmentation, QSM, and individual tree metric computation, are recorded in Table 4. As comparison, manual measurement on the field took between 40 and 120 min depending on tree density. It is important to note that, despite having long computation times, some algorithms can be deployed simultaneously, drastically reducing the global processing time. The specifications of the computer used in this study include a 10* 4.3 GHz CPU, 64 GB of RAM, a GTX 1070 3D card, and an X299 MARK 2 motherboard with a Windows 10 OS.

Table 4. Processing time for each step from point cloud preprocessing to metric estimations and for the full processing of the 60 plots, software used, and the level at which the computation was processed.

STEP	SOFTWARE	ESTIMATED TIME	LEVEL
MLS PLOT SETUP	/	20’	Plot
MLS SCAN	/	15’-25’	Plot
ULS SETUP	/	5’	Plot
ULS SCAN	/	5’	Plot
PREPROCESSING	GEOSLAM connect	60’	Plot
INDIVIDUAL TREE SEGMENTATION	Computree	60’	Plot
QSM	Matlab, TreeQSM	5’	Tree
INDIVIDUAL- AND PLOT-LEVEL TREE METRICS	R, ITSMe, lidR	3’	Plot
FULL INVENTORY COMPUTATION	/	~120 h	60 Plots

3.2 Sampled population

In total, 2,497 trees were measured in the field, of which 661 were beech trees, 112 were oaks, 786 were spruces, 579 were Douglas firs, and 359 pertained to other species among Birch, Hornbeam, Rowan, Hazel, Maple, Linden and Poplar. In addition, MLS detected 2,577 trees of a CBH of at least 20 cm. Of these, 2,212 (i.e., 88.6%) were correctly identified by MLS and matched with their corresponding field observations. A total of 812 individual tree heights were measured in the field using an electronic clinometer. Moreover, 907 trees were detected in the 27 ULS scanned plots.

The mean DBH and height from the total manually measured population were 23.57 cm and 22.55 m, and 23.74 cm and 22.45 m for the correctly matched population.

The mean estimated volume per hectare and number of trees per plot are displayed in Table 5, along with their standard deviations.

Table 5. Plot characteristics regrouped by forest type for mobile laser scanning and field measurements. Mean and standard deviation of volume per hectare (VHA) and number of trees per hectare (NHA) are given for each forest type. SD corresponds to the standard deviation around the mean value.

	STANDS	OAK	BEECH	BEECH AND OAK	SPRUCE	DOUGLAS FIR	SPRUCE AND DOUGLAS' FIR
	Number of plots	4	12	17	12	8	7
MLS	Mean VHA (m^3)	154.28	218.87	168.40	334.32	378.70	355.03
	SD VHA (m^3)	52.21	67.23	74.38	128.36	113.94	142.64
	Mean NHA	446.60	530.60	217.80	378.40	449.10	662.95
	SD NHA	147.43	313.00	75.20	249.75	304.48	412.08
MANUAL MEASUREMENTS	Mean VHA (m^3)	186.75	245.42	225.55	341.34	380.43	349.95
	SD VHA (m^3)	39.27	84.88	64.64	155.45	137.00	173.91
	Mean NHA	415.00	470.00	262.35	424.17	476.25	730.00

	SD NHA	190.18	275.32	63.59	317.30	335.90	433.09

3.3 Tree-level estimations

The individual tree estimation characteristics of the correctly matched population (2212 individuals) are displayed in Table 6.

Table 6. Minimum (MIN), maximum (MAX), mean, and standard deviations (SD) of tree-level metrics estimated by field measurements (FM), mobile laser scanning (MLS), and MLS/unmanned laser scanning (ULS). Units are given in the table for each metric.

		MIN	MAX	MEAN	SD
FM	DBH (cm)	6.36	93.58	23.83	14.53
	Height (m)	5	38.85	22.43	7.68
	Volume (m^3)	0.003	9.18	0.69	1.01
MLS	DBH (cm)	5.44	103.63	23.74	14.30
	Height (m)	5.09	38.33	21.84	7.53
	Volume (m^3)	0.00145	13.45	0.71	1.01
	CPA (m^2)	1.22	214.8	36.71	34.89
	CV (m^3)	3.9	1615.1	214.4	272
MLS/ULS	Height	10	36.9	21.60	6.42
	CPA (m^2)	1.7	215.4	38.63	36.73
	CV (m^3)	7.1	1695.7	233.68	292.8

DBH, diameter at breast height; CPA, Crown projected area; CV, Crown volume

Consistent with several previous studies, we observed that DBH was accurately estimated using MLS data (Fig. 9A). Concerning total height, FM and MLS comparisons were less accurate and precise but with a low bias with an RMSE of 3.7 m (16.3 %) (Fig. 9B). Nevertheless, outliers were still present in the

265 comparison graphs. The results of the analysis by species can be found in table 7. Differences in the
266 quality of the estimations can be made between hardwood and softwood species.

267 When using MLS/ULS tree height as a reference, MLS shows a strong, accurate, estimation with a low
268 bias and RMSE of 1.02 m (5%) (Fig. 9C). Both MLS crown projected area and volume estimations
269 displayed similar trends with a slight underestimation that increases with the size of the crown
270 compared with that estimated by MLS/ULS (Fig. 9D and E). These figures indicate that most MLS
271 observations correlate well with MLS/ULS observations, and a few "outlier" observations mostly drive
272 the differences. These outliers consist of incomplete MLS scanned trees missing parts of the crown due
273 to either occlusion or segmentation errors.

274 **Table 7.** Height, DBH, an and volume bias and standard deviation (SD) by species. A positive difference
275 indicates an overestimation of field measurements (FMs) compared with mobile laser scanning (MLS).
276 Negative numbers indicate an underestimation of FM tree height compared with that of MLS.

SP.	MEAN DBH DIFFERENCE CM) (FM-MLS)	SD	MEAN VOLUME DIFFERENCE(M^3) (FM-MLS	SD	TOTAL NUMBER OF MATCHED TREES	MEAN HEIGHT DIFFERENCE(m) (FM-MLS)	SD	NUMBER OF TREE WITH HEIGHT MEASURED
BEECH	0.55	5.80	0.045	0.55	585	0.83	4.53	211
OAK	2.57	8.87	0.24	0.65	103	2.27	3.83	57
SPRUCE	-0.45	4.89	-0.048	0.36	705	-0.09	2.85	239
DOUGLAS	0.56	3.55	-0.11	0.47	521	-0.17	1.75	161
OTHERS	-1.18	8.69	0.037	0.35	298	0.75	5.51	52

277 Individual tree merchantable wood volumes from FM and MLS measurements display a high RMSE of
278 0.46m^3 (58.2%) and a low bias of -0.048m^3 showing an accurate but imprecise relation (Fig. 9F). The

279 structure of the sampled population, displayed on the side of the graph, shows a high proportion of
280 smaller trees (< 1 m^3) with only a few large individuals.

281 **3.4 Plot-level estimations**

282 The plot-level estimation characteristics of the sampled population calculated based on all field
283 measured trees against all MLS segmented trees are displayed in Table 8.

284 **Table 8**. Minimal (MIN), maximal (MAX), mean values, and standard deviations (SD) around the mean
285 of plot-level metrics for field measurements (FM) and mobile laser scanning (MLS).

		MIN	MAX	MEAN	SD
FM	Plot volume (m^3)	2.1	59.3	28.53	12.94
	Number of trees	11	145	41.62	28.63
	Basal area (m^2)	0.34	4.64	2.53	0.94
MLS	Plot volume (m^3)	1.69	52.81	27.31	12.93
	Number of trees	6	139	39.76	28.13
	Basal area (m^2)	0.29	4.08	2.31	0.89

286

287 FM plot volume and MLS estimated volume display a strong correlation with an RMSE of 8.49 m^3
288 (28.3%) (Fig. 10A). Most plots contained less than 50 trees. Both the total number of trees per plot and
289 summed up basal area were accurately retrieved by MLS despite a few outliers with RMSEs of 6.89
290 (10.1%) and 0.615 (21.7%), respectively (Fig. 10B and C). When analysing further the impact of
291 structure and composition, we noticed that the number of trees identified by the MLS in young

softwood forest tended to be overestimated while it was underestimated in uneven-aged and coppice hardwood forest. Surprisingly, we didn't find any impact from tree density on the proportion of detected and matched trees.

3.4 Inventory-level estimations

The aggregated wood volumes for all matched trees were 1,698.34 m^3 (283.05 m^3/ha) for FM and 1564.05 m^3 (260.67 m^3/ha) for MLS. We identified 2,497 trees manually, of which 2,212 have been matched with a point cloud. DBH and height population structure matched with FM but was slightly lower at the inflexion point for tree height (Fig. 11A and B). When analysing the total estimated volume by stand type, MLS volume tended to be slightly higher than FM volume for hardwood-dominated stands, whereas the opposite was noted for softwood-dominated stands (Fig. 11C).

4 Discussion

4.1 Tree level

4.1.1 DBH

Our estimation of DBH matched the performance of other studies with an RMSE of 5.83 cm and a bias of -0.095 cm (Fig. 9A). Recent MLS studies showed RMSEs ranging from 0.9 to 3.7 cm and bias ranging from -0.44 to 1.27 cm (Liang et al., 2014; Hyyppä et al., 2020; Hartley et al., 2022; Vandendaele et al., 2022; Kükenbrink et al., 2022; Stovall et al., 2023; Balestra et al., 2024b; Kükenbrink et al., 2025). However, a few outliers were identified in our dataset. These can be attributed to either a wrong match between FM and MLS or errors during tree segmentation. The presence of ground vegetation or other solid objects in close proximity to the trunk can hinder the accurate retrieval of DBH using the current method. This may result in overestimation, if such objects are erroneously attributed to the trunk, or underestimation, if occlusion occurs. The application of stronger filters around the base of the stem, or alternatively the use of QSM-derived diameters, may partially mitigate this issue. Furthermore,

315 although the algorithms employed in this study produced promising results, more robust approaches
316 are continuously being developed. Initiatives such as that presented by Murtiyoso et al. (2024) provide
317 valuable guidance to potential MLS users in selecting the most appropriate software for their
318 objectives. Building on this type of work, a comprehensive evaluation of available processing solutions
319 on a large benchmark dataset would be of particular interest. Such an effort would help users
320 determine which methods perform best under specific conditions.

321 Regarding matching error, the polar coordinates measurement, where the angle was determined with
322 a compass and the distance with an electronic clinometer, is also prone to operator and calibration
323 induced errors. At the distance of 18m from the center, a 10° difference ends up in 3.14m horizontal
324 difference.

325 **4.1.2 Tree height**

326 Differences between height estimates are generally higher when comparing FMs and MLS estimates
327 (Fig. 9B) than between MLS and MLS/ULS estimates (Fig. 9C). This could suggest that at least part of
328 these discrepancies may be linked to errors in clinometer-based measurements rather than to LiDAR-
329 derived estimates. Accordingly, MLS/ULS estimates could, in certain contexts, provide a more
330 appropriate reference. In a study evaluating the performance of clinometer estimations, Stereńczak et
331 al. (2019) found that in most cases, tree total height was underestimated compared with reference
332 measurements on felled trees. They also indicated that, unlike most species, oak tended to be
333 overestimated by clinometers. Moreover, Jurjević et al. (2020) reported a 1-m underestimation, on
334 average, using a clinometer.

335 When tree species were analyzed separately, FM tended to report greater total heights for hardwood
336 species compared with MLS, whereas for softwoods, FM generally reported lower values. These
337 differences may stem either from errors in clinometer measurements, such as the operator failing to
338 correctly identify the treetop, or from segmentation artifacts in MLS processing, where higher branches

from neighboring trees are occasionally assigned to smaller individuals. This latter issue is particularly plausible in coniferous stands, as conifers are typically planted at higher densities than deciduous species. Another possible explanation for these disparities is that the hardwood trees were leafless at the time of scanning, whereas the conifers retained their needles. The resulting differences in occlusion affect both tree segmentation and the likelihood of capturing the uppermost portions of the crown, thereby influencing height estimation.

The performance of MLS under leaf-on conditions should nonetheless still be tested in order to study the effect of leaves and vegetation on height estimations. With leaves acting as an optical barrier for the laser beam, we anticipate more occlusion in the canopy during the vegetation period and an overall underestimated MLS height regardless of the species.

4.1.3 Crown area and volume

Crown projected area and volume estimation with the ULS enhanced point cloud didn't change significantly from MLS point cloud (Fig. 8D and E), demonstrating that the selected pattern allowed correct canopy capture and limited occlusion in the higher parts of trees. The few trees for which MLS underestimated crown volume included mostly large oaks and beeches. For these trees, the crown was intricate, and many large branches occluded the top; however, adding ULS to the scan added value in those particular cases. Interestingly, MLS and MLS/ULS crown metrics for coniferous species were largely consistent, despite the dense crown structure leading to incomplete point cloud data in the upper portions of the crown. This consistency may be attributed to the organized layout of coniferous plantations and the relatively regular architecture of their crowns. In general, ULS provided a more complete representation of the crown structure, particularly for the largest tree.

Combining ULS and MLS is valuable under challenging conditions, such as densely populated forests where MLS rays could be quickly occluded by low vegetation, especially in plots populated by tall trees, densely planted coniferous, or during leaf-on conditions. In their study, Liang et al. (2019) found that

ULS better determines tree height than its terrestrial counterpart, while MLS better estimates DBH and stem-related metrics. The two sampling methods could, therefore, benefit from each other as occlusion tends to occur more at the ground and stem levels for ULS, wherein it sometimes misses small trees entirely (Polewski et al., 2019; Donager et al., 2021), whereas this occurs more at the crown and canopy levels with MLS (Liang et al., 2019). When ULS is not feasible, airborne laser scanning (ALS), if available, could complement MLS at a lower resolution. In the study area, ALS data are available across the entire territory. Although less dense than ULS point clouds, the integration of ALS and MLS may enhance the accuracy of height and crown estimations. A thorough evaluation of the potential benefits of such data fusion under similar conditions would be necessary.

4.1.4 Wood volume

By extracting merchantable wood volume from the QSM generated using MLS, we were able to match it with commonly used volume equations (Fig. 9F). Even if the relationship is quite strong, the RMSE remains relatively high. Volume equations were constructed based on a large number of destructive tree measurements to accurately conduct the volume evaluation for large inventories. Their focus is thus on global, rather than local, accuracy and are better suited to estimate total volume at the scale of a forest stand (Chave et al., 2014). MLS estimation is site-specific, while volume equations depend on the initial dataset used to construct them. Servotte (2017) evaluated the accuracy of Dagnelie's spruce equation. Even though they notice an overestimation for small tree and an underestimation for larger one, they showed that the equation performs well for trees between 10 and 280 cm of circumference with less than 8% of mean error.

Some circumstances limiting volume equation performances included broken stems and forking or bent trees. Using two-entry volume equations, which require CBH and tree height, or one entry calibrated equation, which uses stand dominant height, could partially solve these problems. Nevertheless, the use of one-entry equations is often required as height is rarely measured for every sampled tree.

In the present study, we did not have wood volume references from destructive measurements. Further studies should evaluate the overall quality of both MLS and FM estimates in the context presented herein. We expect MLS volume estimates to be more accurate than those of FM, given that Vandendaele et al. (2022) found that MLS stem merchantable wood volume can be as accurate as TLS data. Furthermore, these TLS estimates have shown the potential to be more accurate than allometric equations (Burt et al., 2021).

4.2 Plot level

4.2.1 Wood volume

Regarding plot-level wood volume observations, individual tree errors do not seem to exactly compensate each other as many plot volumes are still over- or underestimated when comparing MLS with volume equation estimations (Fig. 10A).

The total number of trees per plot in Fig. 12 shows that MLS volumes are higher than FM volumes for plots with fewer individual trees (<50 trees). On the other hand, the volume for plots with over 75 trees is, for all but two, estimated to be lower by MLS than by FM, indicating that the impact of forest structure on overall occlusion and on the estimations is not negligible and should be further investigated.

4.2.2 Number of trees

The number of trees detected per plot often varied between MLS and FM (Fig. 10B). One of the causes for such differences is tree positioning error. Some trees located close to the edge of the plot were considered out of range by one method while being incorporated by the other. Another cause is the imprecision of DBH estimations. Depending on the situation, DBH could be slightly over- or underestimated by MLS. Trees with a DBH approximating 20 cm could be added or omitted from the inventory. The last identified cause is inaccurate tree segmentation. Tree segmentation algorithms

sometimes fail to properly identify individual trees from the plot point cloud under challenging conditions. Among these challenging conditions, we mostly identified forked trees, trees with numerous low branches, small trees, and trees growing in particularly dense vegetation (Hartley et al., 2022).

4.2. Basal area

Even with the aforementioned sources of error, the total basal area was accurately estimated (Fig. 10C). In most cases, total basal area of a plot is mostly driven by the biggest trees in this plot, and so is total merchantable wood volume. As these larger trees are more accurately detected and measured by the MLS, the weight they have in plot level estimation induce an overall good plot level accuracy. This phenomenon has also been noted by Holmgren et al. (2019) and Vatandaşlar and Zeybek (2020). Donager et al. (2021) also observed the accurate retrieval of the plot-level total basal area from MLS.

4.3 Whole inventory level

Considering the whole inventory by summing up plots, MLS estimates of the number of trees are close to FM estimates. This could imply that the bigger the inventory scale, the more accurate the estimations. Further statistical testing on a larger number of plots would be necessary to confirm this hypothesis. Nonetheless, MLS total wood volume is estimated 8% lower than FM.

The MLS overestimation of the total number of trees partially stems from bushes and other low and dense vegetation being detected as trees by the segmentation algorithms. While, in our study, these false detections could be removed during the tree-matching process, additional care should be practised if no manually measured tree positions are available during the segmentation process. The use of additional filters applied to tree height or structure could partially solve this problem.

The effective detection rate, when considering matched trees only, was estimated to be 88.6%, which is lower than that of previous studies (>90%) (Chen et al., 2019; Donager et al., 2021; Hartley et al., 2022). More accurate segmentation processes could potentially improve this detection rate.

We noted a difference in the accuracy of the estimations between coniferous and broad leave forest plots regarding total plot wood volume, tree detection, and individual tree heights (Fig. 11 and Tables 3 and 6). These differences could be attributed to MLS accuracy differing among forest types and structures or to FMs errors. In Wallonia, coniferous and broadleaved forests have markedly different structures, with coniferous typically planted in well-organized rows, while broadleaves forest often exhibit a more natural layout with greater natural regeneration. However, the mechanisms by which these profiles influence MLS estimations are not yet well known. While a higher degree of occlusion is likely to be the cause of this difference, further studies on this topic are needed to correctly interpret the results for large-scale MLS forest inventories.

4.4. Considerations regarding MLS integration in NFIs

4.4.1 MLS' limitations

From an operational perspective, while the use of MLS and ULS in large-scale inventories has high potential, their regular deployment in the field is not easy. Both tools are sensitive to wind and rain, and the impact of forest structure and topography on data quality remains unclear. These elements might prove problematic in large-scale NFI, where measurement accuracy will impact overall monitoring. Therefore, understanding their effects under a wide range of situations is necessary. A pre-implementation phase in an NFI based on a large set of plots throughout at least one year could help detect and mitigate the potential sources of error and biases in MLS measurements coming from different forest type, weather conditions and vegetation seasonality.

In addition to these potential issues, additional constraints to the potential use of MLS in NFIs were noticeable during fieldwork. While the quality of the data measured on the plot might be sufficient,

these other constraints bring new challenges and might complicate the correct implementation of MLS in NFI.

The dependence on weather made ensuring a continuous MLS inventory difficult. While the traditional measurement rhythm of 4 plots a day could be met with the MLS scans, scanning 20 plots weekly was often impossible, resulting in an uncertain progression speed. This weather dependency poses planification difficulties for potential NFI crews. The impossibility of reaching and scanning certain plots due to heavy slopes or hazardous terrain prevented the full coverage of our first plot selection by MLS. While this did not cause much of an issue in our study, as we could easily select other plots, it will represent another concern in the context of NFIs. The systematic omission of certain types of forest or topographic profiles will induce a non-negligible bias in the statistical conclusions of NFIs and would be a major issue in an NFI framework. In those situations, strategies to mitigate the induced bias, such as prior studies allowing the estimation of the lost measurements or the development of sub-canopy drone scanning, will need to be developed. Additionally, leaf-on and leaf-off conditions influence the overall quality of measurements across seasons. While the effect of seasonality is less pronounced in coniferous and evergreen forests, it presents greater challenges in deciduous hardwood stands, where occlusion varies substantially throughout the year.

The time needed to process data is also an obstacle to the regular use of MLS technology in NFIs. Many NFI sample forest plots throughout the year alongside computer processing of the data. Processing time issues would then arise if a growing delay between the two would occur. Additionally, several applications and algorithms used needs regular supervision and frequent manual input. Qualified personnel will be needed to oversee the process and intervene in case of errors or exceptions during calculations. This work requires programming knowledge as well as an understanding of the software used. With the development of new automated algorithms and parameter extraction methods parallel to the ongoing development of computer power, processing times are expected to progressively

decrease, lessening this constraint. We also expect more user-friendly models to be developed, thus decreasing the need for highly qualified personnel.

Point cloud data quality can remain a major issue as it could influence the accuracy of the retrieved parameters. A focus should be put on both the impact of data quality on the overall estimations and on the development of more robust algorithms that could cope with lower quality data and potentially incomplete point clouds. Recently, deep learning and AI algorithms have been developed, aiming at either filling incomplete occluded stem and branch sections (Bornand et al., 2024) or generating full trees point cloud from cut portion of the point cloud (Zhang et al., 2025).

4.4.2 MLS' potential

On the other hand, in addition to the tree attributes successfully retrieved by MLS in the present study, several potential attributes are being developed and tested. Tree attributes such as leaf area Index (Zheng et al., 2013), leaf area ratios and foliage distribution (Zhu et al., 2023), and individual tree micro-habitats (Rehush et al., 2018) could be added to the usual dendrometric attributes using the same MLS. The potential also exists to retrospectively measure these new indexes by reprocessing older scans and retroactively monitoring their evolution over time.

In our study, we focused on circular plots with 18-m radii. While this was done from the perspective of comparing MLS with FM, the surface covered by MLS could easily be expanded without drastically increasing the time of the scan. Vandendaele et al. (2024) studied the effect of the acquisition scenario on the accuracy and precision of the estimations. They found that a 20m grid pattern covering 1 hectare gave them the best results.

Furthermore, while the standard Wallonia forest inventory involves three concentric subplots where trees are measured or left out depending on DBH thresholds with smaller trees being measured on a smaller surface than larger trees (Rondeux et al., 2010), the surface scanned by the MLS would be sampled uniformly. This could represent a significant advantage as, on the one hand, the larger the

plot, the more representative it becomes, and, on the other hand, since all trees within the plot would be considered on the same surface, extrapolation to higher levels would be more accurate.

Regarding the overall performance of MLS compared with that of FMs, while FMs have been acquired using traditional means that are well accepted for forest inventory purposes, these measurements are not without their source of errors. Taking this into account, MLS errors should not be considered as the differences between MLS estimates and those of traditional measurements. This is specifically the case for volume estimations. Only tedious destructive measurements would serve as a proper reference and allow us to demonstrate whether MLS performs better than allometric equations.

5 Conclusion

This study evaluated the capacity of MLS to build large-scale forest inventories in the context of NFIs and RFIs by comparing estimates at three levels: individual tree, plot, and inventory levels. A comparison of the results of MLS estimations with FM and MLS/ULS attributes gave encouraging results for the most common metrics retrieved by forest inventories on a large scale. We also discussed coupling ULS data to MLS to augment the 3D point cloud and derive more accurate estimates. However, this might prove challenging in an operational context.

Collectively, MLS is a highly promising technology. It has the potential to revolutionise forest inventories by enabling accurate measurements. MLS also increases the number of potential attributes and metrics that can be estimated from a forest plot. In addition, it may allow for larger plot sizes, and therefore a greater number of trees to be measured in the field.

However, further investigations are required, notably during leaf-on conditions, to ensure the robustness of the approach and to explore more complex metrics. Additional attention must be paid to reference wood volume measurement and the impact of forest type and structure on MLS estimations.

Acknowledgements

This research was founded by the interreg GR W.A.V.E. project (https://wave-gr.eu/en/). The authors would like to thank Cedric Geerts for his active participation during the field survey and his help with data processing. We are also grateful to Sebastion Bauwens and Bastien Vandendaele for the numerous exchanges during the different stages of this research. We would also like to acknowledge the Wallonia DNF, particularly the NFI cell, which provided us access to their plots.

Funding

This research was supported by the "quinquennial plan of forestry research" of Wallonia's DNF and by the university of Liège, faculty of Gembloux Agro-Bio Tech.

CRediT author contribution statement

Justin Holvoet; Conceptualization; Methodology; Software; Formal analysis; Investigation; Data Curation; Writing - Original Draft; Visualization

Nicolas Latte; Conceptualization; Writing - Review & Editing; Supervision

Jérôme Perin; Conceptualization; Writing - Review & Editing; Supervision

Jean-François Bastin; Investigation; Resources

Hugo Delame; Investigation; Resources; Data Curation

Daniel Kükenbrink; Conceptualization; Software; Resources; Writing - Review & Editing; Supervision

Philippe Lejeune; Project administration, Funding acquisition, Supervision; Conceptualization; Writing - Review & Editing; Supervision

Data availability statement

546 The data presented in this study may be available upon reasonable request from the corresponding
547 author.

548 # References

549 Astrup, R., Ducey, M.J., Granhus, A., Ritter, T., Von Lüpke, N., 2014. Approaches for estimating stand-
550 level volume using terrestrial laser scanning in a single-scan mode. Can. J. For. Res. 44, 666–676.
551 https://doi.org/10.1139/cjfr-2013-0535.

552 Balestra, M., Marselis, S., Sankey, T.T., Cabo, C., Liang, X., Mokroš, M., Peng, X., Singh, A., Stereńczak, K.,
553 Vega, C., Vincent, G., Hollaus, M., 2024a. LiDAR Data Fusion to Improve Forest Attribute
554 Estimates: A Review. Curr. For. Rep. 10, 281–297. https://doi.org/10.1007/s40725-024-00223-7

555 Balestra, M., Cabo, C., Murtiyoso, A., Vitali, A., Alvarez-Taboada, F., Cantero-Amiano, A., Bolaños, R.,
556 Laino, D., Pierdicca, R., 2024b. Advancing forest inventory: a comparative study of low-cost MLS
557 lidar device with professional laser scanners. Int. Arch. Photogramm. Remote Sens. Spatial Inf.
558 Sci. XLVIII-2/W8-2024, 9–15. https://doi.org/10.5194/isprs-archives-XLVIII-2-W8-2024-9-2024

559 Bienert, A., Georgi, L., Kunz, M., Von Oheimb, G., Maas, H.-G., 2021. Automatic extraction and
560 measurement of individual trees from mobile laser scanning point clouds of forests. Ann. Bot.
561 128, 787–804. https://doi.org/10.1093/aob/mcab087.

562 Burt, A., Vicari, M.B., Coughlin, I., Meir, P., Rowland, L., Disney, M., 2021. New insights into large
563 tropical tree mass and structure from direct harvest and terrestrial lidar. R. Soc. Open Sci. 8, 19.
564 https://doi.org/10.1098/rsos.201458.

565 Cabo, C., Del Pozo, S., Rodríguez-Gonzálvez, P., Ordóñez, C., González-Aguilera, D., 2018. Comparing
566 terrestrial laser scanning (TLS) and wearable laser scanning (WLS) for individual tree modeling at
567 plot level. Remote Sens. 10, 540. https://doi.org/10.3390/rs10040540.

568 Calders, K., Adams, J., Armston, J., Bartholomeus, H., Bauwens, S., Bentley, L.P., Chave, J., Danson,
569 F.M., Demol, M., Disney, M., Gaulton, R., Krishna Moorthy, S.M., Levick, S.R., Saarinen, N.,
570 Schaaf, C., Stovall, A., Terryn, L., Wilkes, P., Verbeeck, H., 2020. Terrestrial laser scanning in forest
571 ecology: Expanding the horizon. Remote Sens. Environ. 251, 112102.
572 https://doi.org/10.1016/j.rse.2020.112102.

573 Chave, J., Réjou-Méchain, M., Búrquez, A., Chidumayo, E., Colgan, M.S., Delitti, W.B.C., Duque, A., Eid,
574 T., Fearnside, P.M., Goodman, R.C., Henry, M., Martínez-Yrízar, A., Mugasha, W.A., Muller-
575 Landau, H.C., Mencuccini, M., Nelson, B.W., Ngomanda, A., Nogueira, E.M., Ortiz-Malavassi, E.,
576 Pélissier, R., Ploton, P., Ryan, C.M., Saldarriaga, J.G., Vieilledent, G., 2014. Improved allometric
577 models to estimate the aboveground biomass of tropical trees. Glob. Chang. Biol. 20, 3177–
578 3190. https://doi.org/10.1111/gcb.12629.

579 Chen, S., Liu, H., Feng, Z., Shen, C., Chen, P., 2019. Applicability of personal laser scanning in forestry
580 inventory. PLOS ONE. 14, e0211392. https://doi.org/10.1371/journal.pone.0211392.

581 Corona, P., Chirici, G., McRoberts, R.E., Winter, S., Barbati, A., 2011. Contribution of large-scale forest
582 inventories to biodiversity assessment and monitoring. Forest Ecol. Manag. 262, 2061–2069.
583 https://doi.org/10.1016/j.foreco.2011.08.044.

584 Dagnelie, P., Palm, R., Rondeux, J., 1999. Tables de cubage des arbres et des peuplments forestier,
585 seconde édition. Les Presses Agronomiques de Gembloux, G. (Ed.). Belgique, Gembloux.

586 Di Stefano, F., Chiappini, S., Gorreja, A., Balestra, M., Pierdicca, R., 2021. Mobile 3D scan LiDAR: A
587 literature review. Geom. Nat. Hazards Risk. 12, 2387–2429.
588 https://doi.org/10.1080/19475705.2021.1964617.

589 Donager, J.J., Sánchez Meador, A.J., Blackburn, R.C., 2021. Adjudicating perspectives on forest
590 structure: How do airborne, terrestrial, and mobile lidar-derived estimates compare? Remote
591 Sens. 13, 2297. https://doi.org/10.3390/rs13122297.

592 Fekry, R., Yao, W., Cao, L., Shen, X., 2022. Ground-based/UAV-LiDAR data fusion for quantitative
593 structure modeling and tree parameter retrieval in subtropical planted forest. Forest Ecosystems
594 9, 100065. https://doi.org/10.1016/j.fecs.2022.100065

595 Hackenberg, J., Spiecker, H., Calders, K., Disney, M., 2015. SimpleTree —An efficient open source tool
596 to build tree models from TLS clouds. Forests. 6, 51. https://doi.org/DOI.
597 https://doi.org/10.3390/f6114245.

598 Hartley, R.J.L., Jayathunga, S., Massam, P.D., De Silva, D., Estarija, H.J., Davidson, S.J., Wuraola, A.,
599 Pearse, G.D., 2022. Assessing the potential of backpack-mounted mobile laser scanning systems
600 for tree phenotyping. Remote Sens. 14, 3344. https://doi.org/10.3390/rs14143344.

601 Hopkinson, C., Chasmer, L., Young-Pow, C., Treitz, P., 2004. Assessing forest metrics with a ground-
602 based scanning lidar. Can. J. For. Res. 34, 573–583. https://doi.org/10.1139/x03-225.

603 Huang, H., Li, Z., Gong, P., Cheng, X., Clinton, N., Cao, C., Ni, W., Wang, L., 2011. Automated methods
604 for measuring DBH and tree heights with a commercial scanning lidar. Photogramm. Eng.
605 Remote Sens. 77, 219–227. https://doi.org/10.14358/PERS.77.3.219.

606 Hyyppä, E., Yu, X., Kaartinen, H., Hakala, T., Kukko, A., Vastaranta, M., Hyyppä, J., 2020. Comparison of
607 backpack, handheld, under-canopy UAV, and above-canopy UAV laser scanning for field
608 reference data collection in boreal forests. Remote Sens. 12, 3327.
609 https://doi.org/10.3390/rs12203327.

610 Jin, S., Sun, X., Wu, F., Su, Y., Li, Y., Song, S., Xu, K., Ma, Q., Baret, F., Jiang, D., Ding, Y., Guo, Q., 2021.
611 Lidar sheds new light on plant phenomics for plant breeding and management: Recent advances
612 and future prospects. ISPRS J. Photogramm. 171, 202–223.
613 https://doi.org/10.1016/j.isprsjprs.2020.11.006.

614 Jurjević, L., Liang, X., Gašparović, M., Balenović, I., 2020. Is field-measured tree height as reliable as
615 believed – Part II, A comparison study of tree height estimates from conventional field

measurement and low-cost close-range remote sensing in a deciduous forest. ISPRS J. Photogramm. 169, 227–241. https://doi.org/10.1016/j.isprsjprs.2020.09.014.

Kovácsová P., Antalová M. 2010 - Precision Forestry - definition and technologies, Pregledničlanci . Reviews 11-12: 603-611.

Kükenbrink, D., Marty, M., Bösch, R., Ginzler, C., 2022. Benchmarking laser scanning and terrestrial photogrammetry to extract forest inventory parameters in a complex temperate forest. Int. J. Appl. Earth Obs. Geoinf. 113, 102999. https://doi.org/10.1016/j.jag.2022.102999.

Kükenbrink, D., Marty, M., Rehush, N., Abegg, M., Ginzler, C., 2025. Evaluating the potential of handheld mobile laser scanning for an operational inclusion in a national forest inventory – A Swiss case study. Remote Sensing of Environment 321, 114685. https://doi.org/10.1016/j.rse.2025.114685

Liang, X., Hyyppä, J., Kaartinen, H., Holopainen, M., Melkas, T., 2012. Detecting changes in forest structure over time with bi-temporal terrestrial laser scanning data. IJGI. 1, 242–255. https://doi.org/10.3390/ijgi1030242.

Liang, X., Hyyppa, J., Kukko, A., Kaartinen, H., Jaakkola, A., Yu, X., 2014. The use of a mobile laser scanning system for mapping Large Forest plots. IEEE Geosci. Remote Sensing Lett. 11, 1504–1508. https://doi.org/10.1109/LGRS.2013.2297418.

Liang, X., Wang, Y., Pyörälä, J., Lehtomäki, M., Yu, X., Kaartinen, H., Kukko, A., Honkavaara, E., Issaoui, A.E.I., Nevalainen, O., Vaaja, M., Virtanen, J.-P., Katoh, M., Deng, S., 2019. Forest in situ observations using unmanned aerial vehicle as an alternative of terrestrial measurements. For. Ecosyst. 6, 20. https://doi.org/10.1186/s40663-019-0173-3.

Luoma, V., Saarinen, N., Wulder, M., White, J., Vastaranta, M., Holopainen, M., Hyyppä, J., 2017. Assessing precision in conventional field measurements of individual tree attributes. Forests. 8, 38. https://doi.org/10.3390/f8020038.

640 Othmani, A., Piboule, A., Krebs, M., Stolz, C., 2011. Towards Automated and Operational Forest
641 Inventories with T-Lidar 10.

642 Panagiotidis, D., Abdollahnejad, A., Slavík, M., 2022. 3D point cloud fusion from UAV and TLS to assess
643 temperate managed forest structures. Int. J. Appl. Earth Obs. Geoinf. 112, 102917.
644 https://doi.org/10.1016/j.jag.2022.102917.

645 Polewski, P., Yao, W., Cao, L., Gao, S., 2019. Marker-free coregistration of UAV and backpack LiDAR
646 point clouds in forested areas. ISPRS J. Photogramm. 147, 307–318.
647 https://doi.org/10.1016/j.isprsjprs.2018.11.020.

648 Raumonen, P., Kaasalainen, M., Åkerblom, M., Kaasalainen, S., Kaartinen, H., Vastaranta, M.,
649 Holopainen, M., Disney, M., Lewis, P., 2013. Fast automatic precision tree models from
650 terrestrial laser scanner data. Remote Sens. 5, 491–520. https://doi.org/10.3390/rs5020491.

651 Raumonen, P., and Akerblom, M. 2022. InverseTampere/TreeQSM. Version 2.4.1 Available from
652 https://github.com/InverseTampere [accessed 11 June 2022]

653 Rehush, N., Abegg, M., Waser, L.T., Brändli, U.-B., 2018. Identifying tree-related microhabitats in TLS
654 point clouds using machine learning. Remote Sens. 10, 1735.
655 https://doi.org/10.3390/rs10111735.

656 Rondeux, J., Lecomte, H., Latte, N., Hébert, J., 2010. L'inventaire forestier permanent de la Région
657 wallonne: Bilan de 15 ans d'un outil aux multiples fonctions. Forêt Nat., 26–33.

658 Schneider, R., Calama, R., Martin-Ducup, O., 2020. Understanding tree-to-tree variations in stone pine
659 (Pinus pinea L.) cone production using terrestrial laser scanner. Remote Sens. 12, 173.
660 https://doi.org/10.3390/rs12010173.

661 Stereńczak, K., Mielcarek, M., Wertz, B., Bronisz, K., Zajączkowski, G., Jagodziński, A.M., Ochał, W.,
662 Skorupski, M., 2019. Factors influencing the accuracy of ground-based tree-height

663 measurements for major European tree species. J. Environ. Manage. 231, 1284–1292.
664 https://doi.org/10.1016/j.jenvman.2018.09.100.

665 Stovall, A.E.L., MacFarlane, D.W., Crawford, D., Jovanovic, T., Frank, J., Brack, C., 2023. Comparing
666 mobile and terrestrial laser scanning for measuring and modelling tree stem taper. For. Int. J.
667 Forest Res. 96, 705–717. https://doi.org/10.1093/forestry/cpad012.

668 Tansey, K., Selmes, N., Anstee, A., Tate, N.J., Denniss, A., 2009. Estimating tree and stand variables in a
669 Corsican Pine woodland from terrestrial laser scanner data. Int. J. Remote Sens. 30, 5195–5209.
670 https://doi.org/10.1080/01431160902882587.

671 Terryn, L., Calders, K., Åkerblom, M., Bartholomeus, H., Disney, M., Levick, S., Origo, N., Raumonen, P.,
672 Verbeeck, H., 2023. Analysing individual 3D tree structure using the R package ITSMe. Methods
673 Ecol. Evol. 14, 231–241. https://doi.org/10.1111/2041-210X.14026.

674 Tomppo, E., Gschwantner, T., Lawrence, M., McRoberts, R.E. (Eds.), 2010. National Forest Inventories:
675 Pathways for Common Reporting. Springer Netherlands, Dordrecht.
676 https://doi.org/10.1007/978-90-481-3233-1.

677 Vandendaele, B., Fournier, R.A., Vepakomma, U., Pelletier, G., Lejeune, P., Martin-Ducup, O., 2021.
678 Estimation of northern hardwood forest inventory attributes using UAV Laser Scanning (ULS):
679 Transferability of laser scanning methods and comparison of automated approaches at the tree-
680 and stand-level. Remote Sens. 13, 2796. https://doi.org/10.3390/rs13142796.

681 Vandendaele, B., Martin-Ducup, O., Fournier, R.A., Pelletier, G., Lejeune, P., 2022. Mobile laser
682 scanning for estimating tree structural attributes in a temperate hardwood forest. Remote Sens.
683 14, 4522. https://doi.org/10.3390/rs14184522.

684 Vatandaşlar, C., Zeybek, M., 2020. Application of handheld laser scanning technology for forest
685 inventory purposes in the NE Turkey. Turk J. Agric For. 44, 229–242. https://doi.org/10.3906/tar-
686 1903-40.

687 Vidal, C., Alberdi, I.A., Hernández Mateo, L., Redmond, J.J. (Eds.), 2016. National Forest Inventories.
688 Springer International Publishing, Cham. https://doi.org/10.1007/978-3-319-44015-6.

689 Wallace, L., Lucieer, A., Watson, C., Turner, D., 2012. Development of a UAV-LiDAR system with
690 application to forest inventory. Remote Sens. 4, 1519–1543. https://doi.org/10.3390/rs4061519.

691 Yu, X., Liang, X., Hyyppä, J., Kankare, V., Vastaranta, M., Holopainen, M., 2013. Stem biomass
692 estimation based on stem reconstruction from terrestrial laser scanning point clouds. Remote
693 Sens. Lett. 4, 344–353. https://doi.org/10.1080/2150704X.2012.734931.

694 Yun, T., Cao, L., An, F., Chen, B., Xue, L., Li, W., Pincebourde, S., Smith, M.J., Eichhorn, M.P., 2019.
695 Simulation of multi-platform LiDAR for assessing total leaf area in tree crowns. Agric. Forest
696 Meteorol. 276–277, 107610. https://doi.org/10.1016/j.agrformet.2019.06.009.

697 Zhu, Y., Li, D., Fan, J., Zhang, H., Eichhorn, M.P., Wang, X., Yun, T., 2023. A reinterpretation of the gap
698 fraction of tree crowns from the perspectives of computer graphics and porous media theory.
699 Front. Plant Sci. 14, 1109443. https://doi.org/10.3389/fpls.2023.1109443.

Figure captions

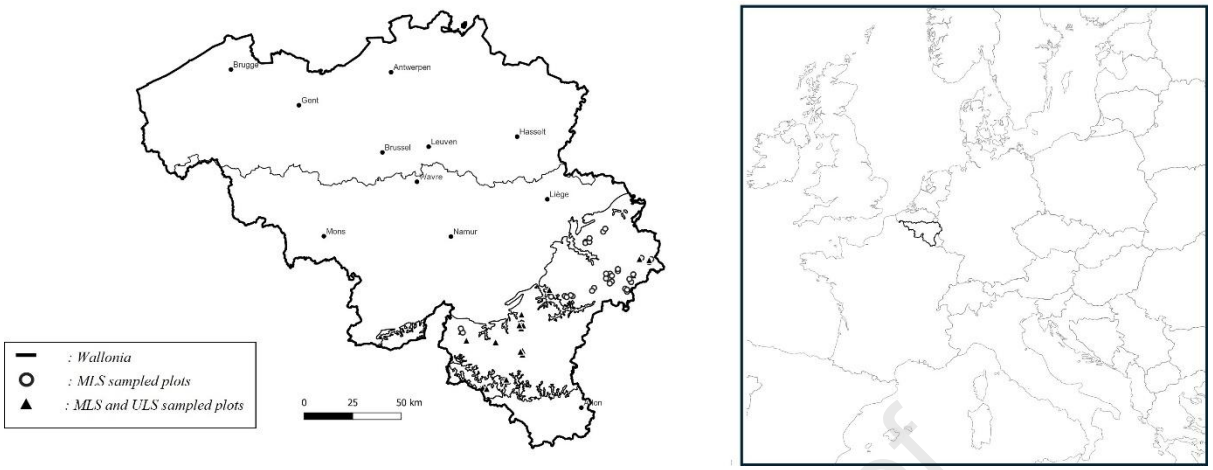

Figure 1. Map of Wallonia displaying the study plots where mobile and unmanned laser scanning were conducted. Right: Location of Wallonia within Europe. Left: Location of the plots within Wallonia.

Figure 2. Picture taken on the scanned plots. Old spruce forest (A), Old beech and oak forest (B), Young spruce forest (C), Young beech forest (D).

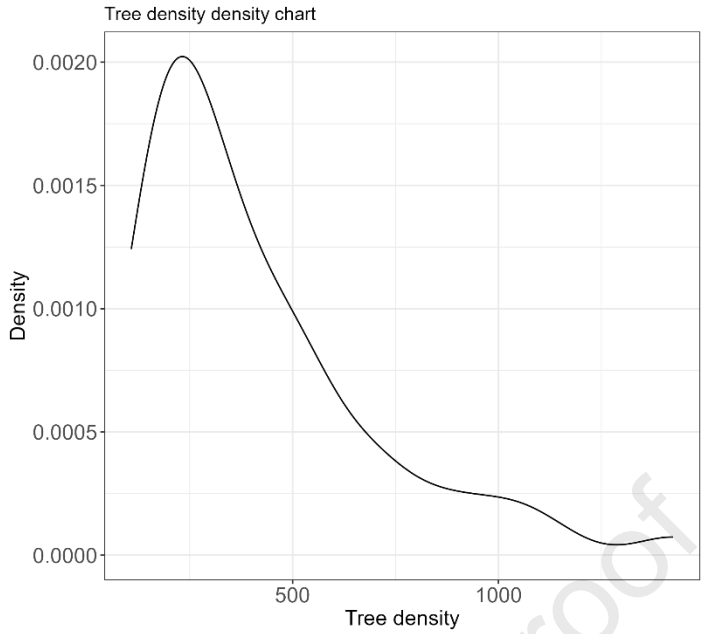

Figure 3. Density graph of the density of tree per plot in the sampled plots.

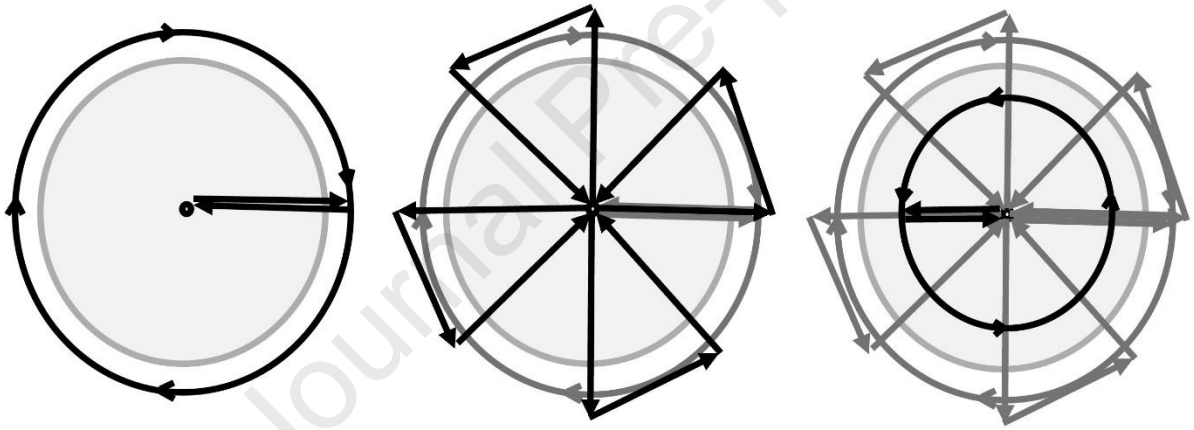

Figure 4. Walking pattern followed during the mobile laser scanning of plots. Black lines indicate, from left to right, the path taken; grey line indicates the path already walked; black dot indicates both the centre of the plot and the start and end points of the scan; the lighter grey circle delimits the plot area; the grey circle represents the surveyed plot.

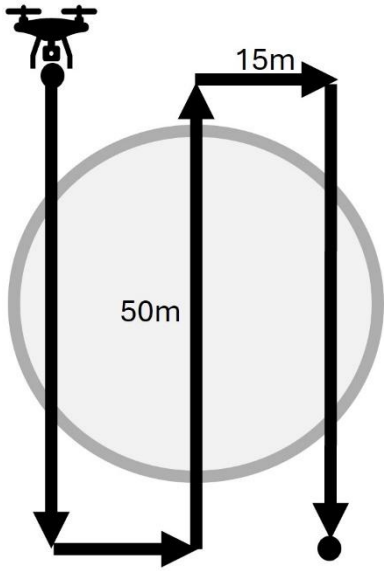

Figure 5. Flight pattern followed by the drone during unmanned laser scanning starting from the top left and ending at the bottom right. Arrows show the acquisition pattern and direction. The grey circle delimits the surveyed plot area.

Figure 6. Fusion of unmanned (ULS) and mobile laser scanning (MLS) point clouds. A: Trench cut in the MLS point cloud (1.5 m wide). B: Trench cut in the ULS point cloud (1.5 m wide). C: Fusion of MLS and ULS point clouds.

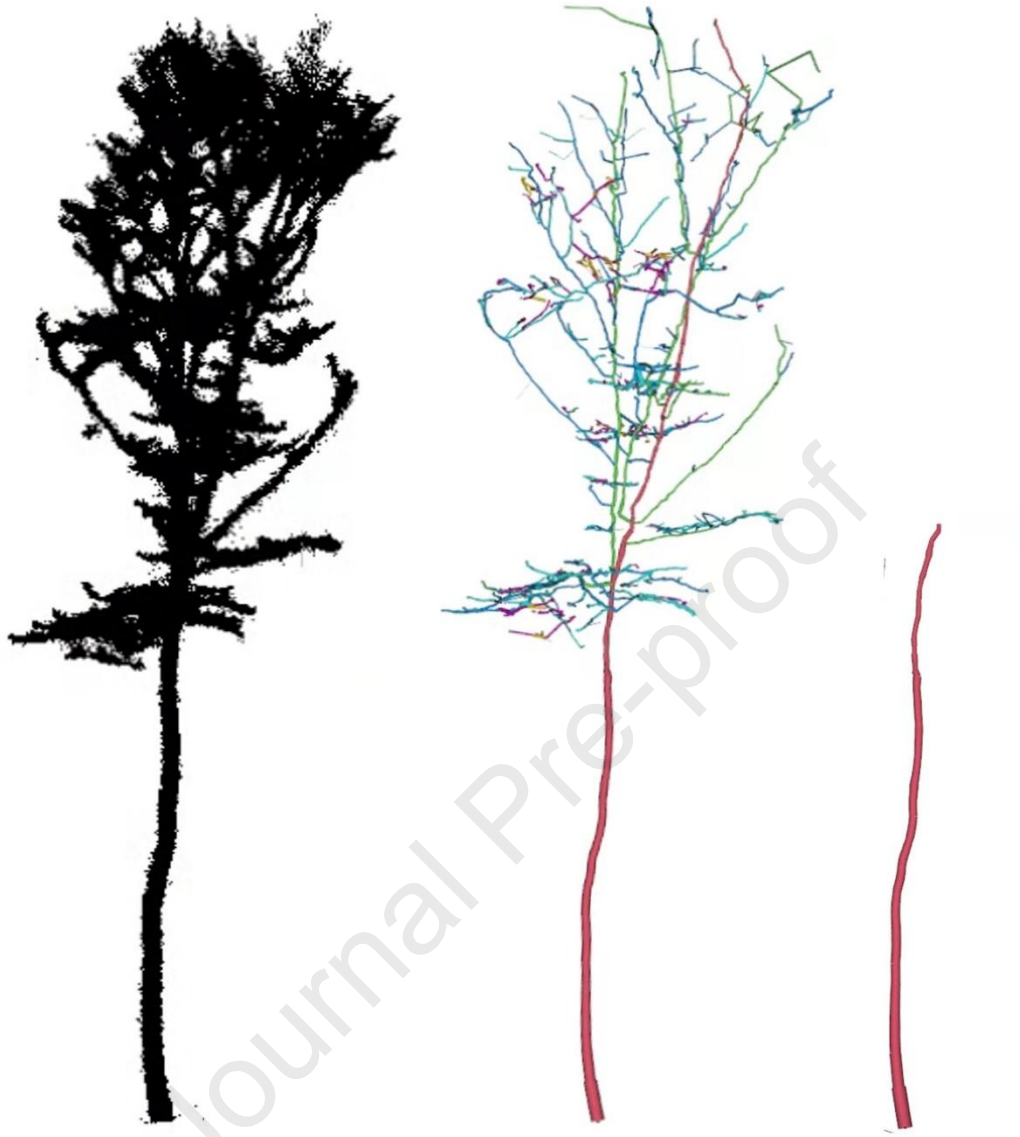

Figure 7. Illustration of quantitative structural model (QSM) and merchantable wood volume estimation using QSMs. Left: individual tree point cloud, middle: total tree QSM, right: merchantable stem volume QSM.

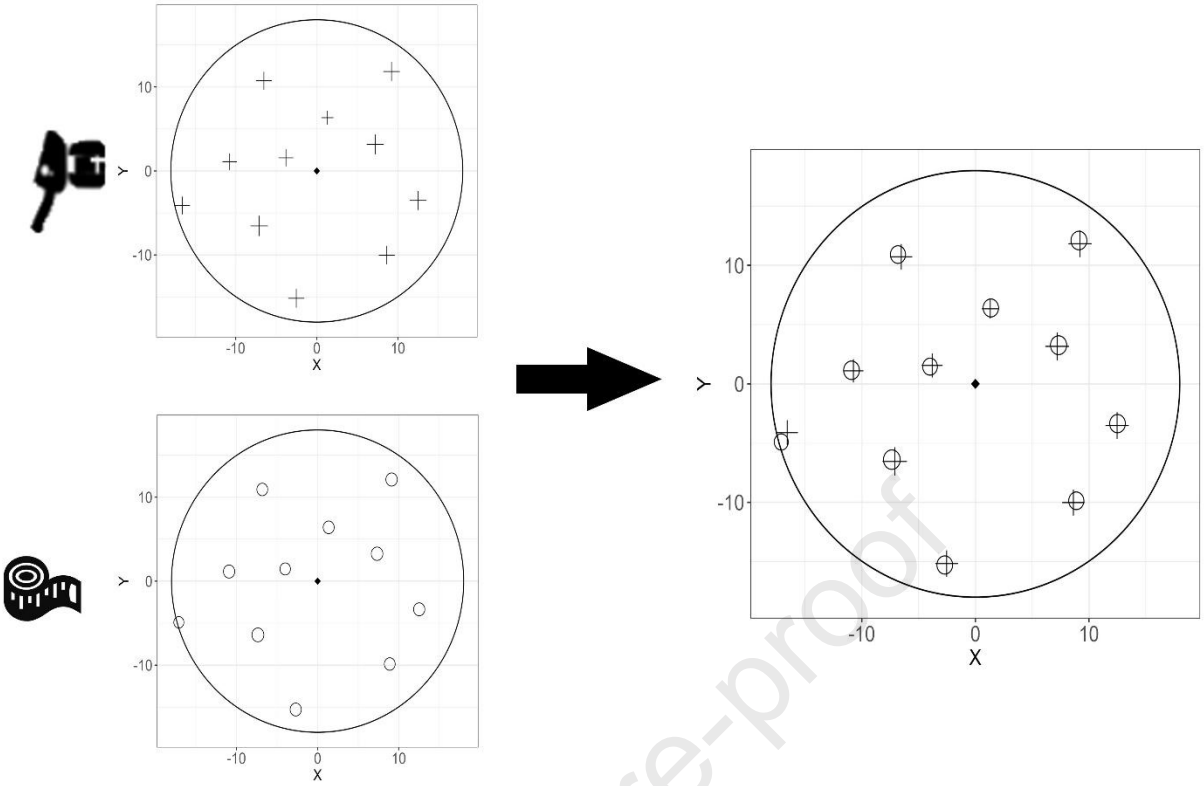

Figure 8. Tree-matching method illustration. Top left: Tree map built using mobile laser scanning (MLS). Bottom left: Tree map built using manual measurements. Right: Tree map alignment. Crosses represent MLS-identified trees; circles represent manually-identified trees.

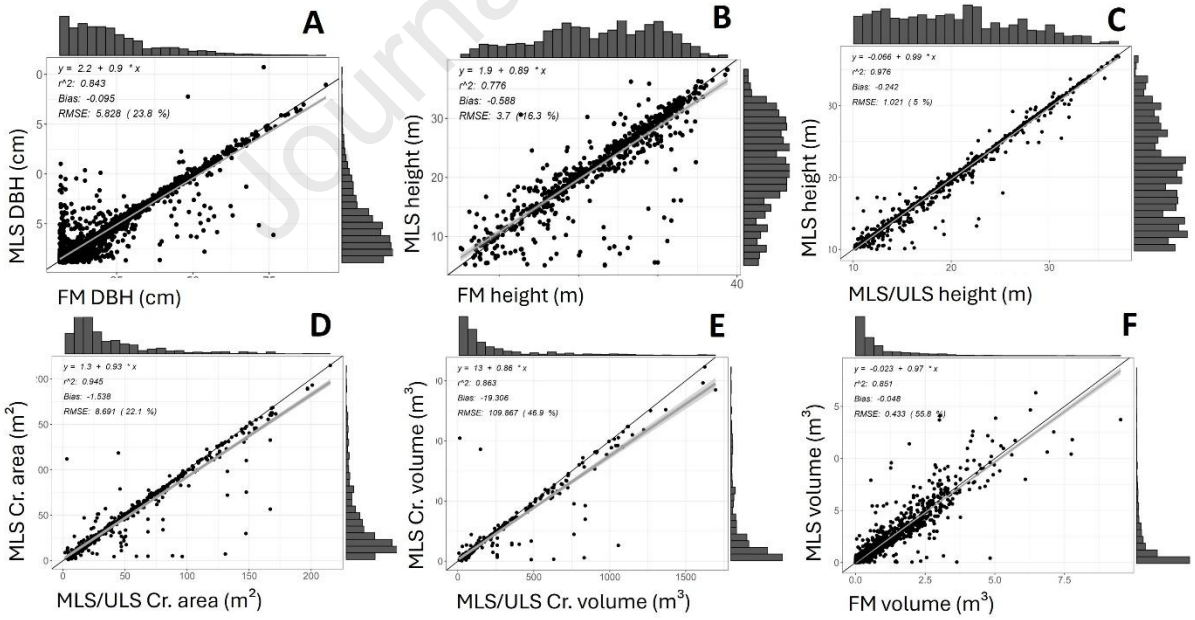

Figure 9. Single tree metric estimation comparison between mobile laser scanning (MLS) and reference measurements. Each point represents an individual tree. The dark grey line represents the linear regression between reference measurements and MLS measurements; its equation, r^2, bias, RMSE, and RMS% are shown in the top left corner. The light grey area represents the confidence interval around the linear regression. The histograms on the side correspond to the population

distribution.FM = Field measurement, MLS/ULS = mobile laser scanning enhanced by unmanned laser scanning, Cr. = Crown.

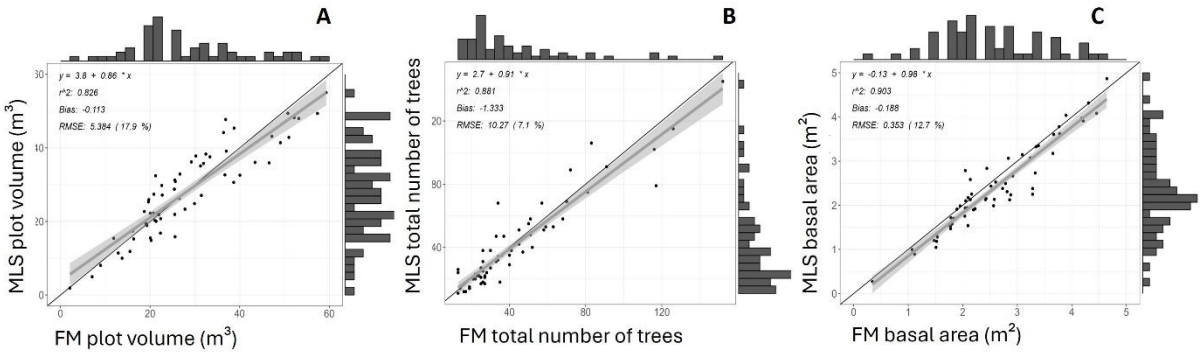

Figure 10. Plot level estimations. Each point represents one 0.1-ha circular plot surveyed manually and by mobile laser scanning (MLS). The dark grey line represents the linear regression between field measurements (FMs) and MLS measurements; its equation, r^2, bias, RMSE, and RMS% are shown in the top left corner. The light grey area represents the confidence interval around the linear regression. The histograms on the side correspond to the population distribution.

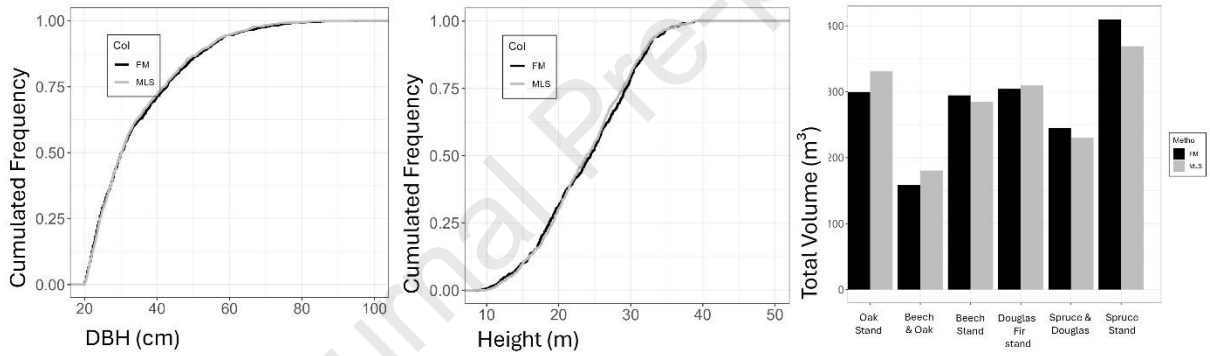

Figure 11. Whole inventory interpretation graphs. Left: cumulated frequency of diameter at breast height (DBH), middle: cumulated frequency of tree total height. The black line represents field measurements; the grey line represents the mobile laser scanning (MLS)-identified population. Right: total volume per forest type. The forest type is defined according to Wallonia's regional forest inventory definition (Rondeux and Lecomte, 2010).

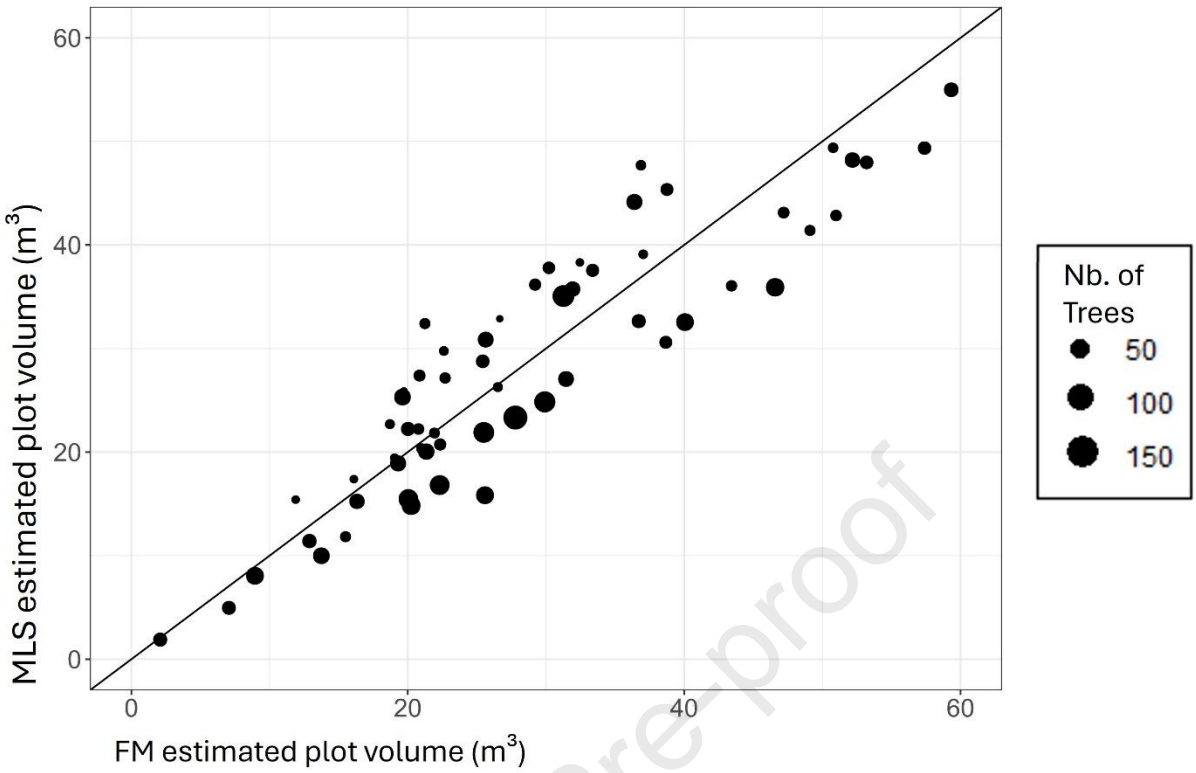

Figure 12. Mobile laser scanning (MLS) and field measurement (FM) plot-level wood volume comparison. The size of the points corresponds to the number of trees per plot identified during FMs. The black line represents the 1:1 line between FM and MLS estimations.

- We retrieved traditional NFI attributes within 60 0.1ha plots using MLS.
- With the same methods, MLS accuracy differs between hardwood and softwood forests.
- Forest structure influences the estimation of total plot wood volume.
- In leaf of conditions, ULS didn't allow a more precise tree height estimation

Declaration of interests

☒ The authors declare that they have no known competing financial interests or personal relationships that could have appeared to influence the work reported in this paper.

☐ The authors declare the following financial interests/personal relationships which may be considered as potential competing interests: